Estimation of Brain Internal Structures by Deforming Brain Atlas Using Finite Element Method

Kaoru Kobayashi[1], Ken'ich Morooka[1], Yasushi Miyagi[2], Takaichi Fukuda[3]
Tokuo Tsuji[1], Ryo Kurazume[1], and Kazuhiro Samura[4]

***Abstract*— This paper presents a method for estimating the internal structures of a patient brain by deforming a standard brain atlas. Conventional deformation methods need several landmarks from the brain surface contour to fit the atlas to the patient brain shape. However, since the number and shapes of small sulci on the brain surface are different from each other, the determination of the accurate correspondence between small sulcus is difficult for experienced neurosurgeons. Moreover, the relationship between the surface shape and internal structure of the brain is unclear. Therefore, even if the deformed atlas is fitted to the patient brain shape exactly, the use of the deformed atlas does not always guarantee the reliable estimation of the internal structure of the patient brain. To solve these problems, we propose a new method for estimate the internal structure of a patient brain by the finite element method (FEM). In the deformation, our method select the landmarks from the contours of both the brain surface and the detectable internal structures from MR images.**

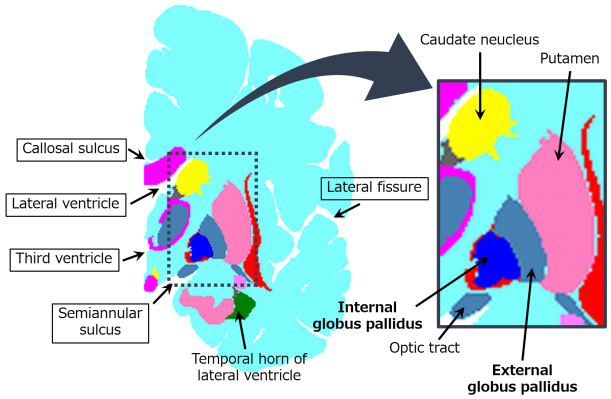

Fig. 1. Brain atlas with the name of internal brain structure and the sulcus (enclosed)

I. INTRODUCTION

Deep brain stimulation (DBS) is a surgical treatment for involuntary movement such as Parkinson's disease and dystonia. During DBS surgery, an electrode is inserted deeply into target structures of the left and right sides of a patient brain. Through the electrode, an electrical stimulus is delivered to the target structures in the brain. The target structures depending on the disorder include internal globus pallidus (IGP) and external globus pallidus (EGP). Since these target structures are very small, a surgeon identifies the accurate location of the structure to accurately insert the electrode into the structure. However, the target structures are difficult to detected clearly from MR images [1].

One solution for this problem is to use a brain atlas[2], which is the collection of the sketches of brain sections. Each sketch consists of the boundaries of the anatomic brain structures. Fig. 1 shows one example of the coronal sections of the atlas. Using the atlas, the internal structures of the patient brain is estimated by deforming the atlas to fit the brain surface of the atlas to that of the patient brain. There are several commercial systems for atlas-assisted estimation of the patient brain structure using MR images. In the system, piecewise linear deformation is used to deform the atlas. However, the accuracy of the deformation is not good because of its lack of deformation degree of freedom.

Recent works have been paid attention to non-linear deformation methods using radial bases functions (RBF) [3], [4], [5] because of its high deformation degree compared with the linear deformation. In the non-linear deformation, several landmarks are manually selected from the brain surface of the atlas. The atlas is deformed smoothly by RBF interpolation while moving the landmarks to their corresponding point on the patient brain. The accuracy of the non-linear deformation depends on the correspondence between the atlas and the patient brain from the landmarks. However, since the number and shapes of small sulci on the brain surface are different from each other, the determination of the accurate correspondence between small sulcus is difficult for experienced neurosurgeons. Moreover, the relationship between the surface shape and internal structure of the brain is unclear. Therefore, even if the deformed atlas is fitted to the patient brain shape exactly, the use of the deformed atlas does not always guarantee the reliable estimation of the internal structure of the patient brain.

To solve these problems, we propose a new method for estimate the internal structure of a patient brain by the finite element method (FEM). In the deformation, our

This work was supported in part by Grant-in-Aid for Scientific Research JSPS KAKENHI Grant Numbers 24390345, 26560262, and Grant-in-Aid for Research on Measures for Intractable Diseases : 201024171A from Ministry of Health, Labour and Welfare, Japan.

[1]K. Kobayashi, K. Morooka, T. Tsuji, and R. Kurazume are with Graduate School of Information Science and Electrical Engineering, Kyushu University, 744 Motooka Nishi-ku Fukuoka, Japan
k_kobayashi at irvs.ait.kyushu-u.ac.jp morooka at irvs.ait.kyushu-u.ac.jp

[2]Y. Miyagi is with Department of Neurosurgery, Kaizuka Hospital, 7-7-27 Hakozaki Higashi-ku Fukuoka, Japan

[3]T. Fukuda is with Graduate School of Medical Sciences, Kumamoto University, 1-1-1 Honjo Chuo-ku Kumamoto, Japan

[4]K. Samura is with Department of Neurosurgery, Fukuoka University, 7-45-1 Nanakuma Jonan-ku Fukuoka, Japan

978-1-4244-7929-0/14/$26.00 ©2014 IEEE

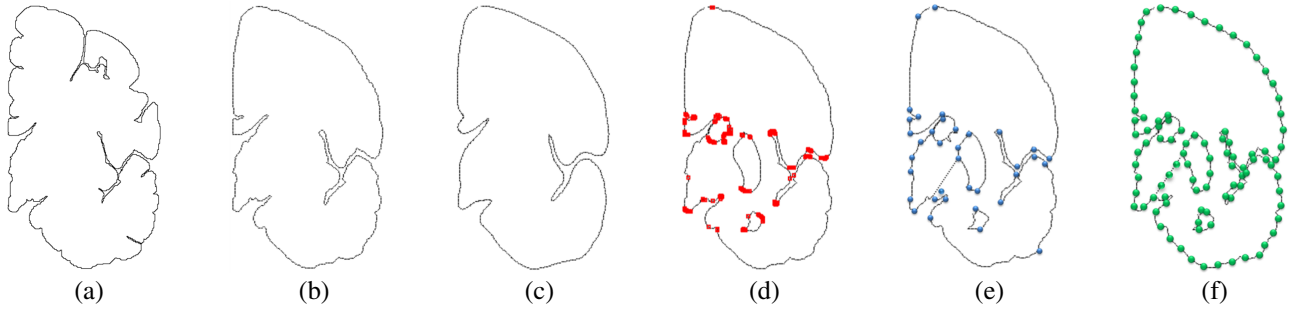

Fig. 2. Landmark selection: (a) original brain outer surface of the atlas in Fig. 1; (b) approximated shape extracted by hand; (c) final simplified brain outer surface; (d)the points at parts of high curvature of the brain outer surface; (e) initial landmarks selected based on the point in (d); (e) final landmarks.

method select the landmarks from the contours of both the brain surface and the detectable internal structures from MR images.

II. METHOD

The target structure in our method is IGP and EGP which are the specific structures to be stimulated for Parkinson's disease and dystonia. An experienced neurosurgeons select the coronal section of the atlas (Fig. 1) which include IGP and EGP, and the corresponding coronal image of a patient. One section of the atlas contains the set of the contours of the brain surface and internal structures. Each contour is composed of the points on the contours. Here, the outer surface of a brain includes the brain surface and the contours of several structures in the brain such as lateral ventricle and third ventricle.

A. Shape approximation of brain outer surface

As described above, the number and shapes of small sulci vary considerably across individuals. On the contrary, major sulci and gyri are common anatomical structures in human brains. To determine the correspondence between the atlas and the patient brain, the shape of the brain outer surface is approximated by smoothing the whole outer surface while keeping the shape of the major sulci and gyri. We use as the major sulci and gyri Callosal sulcus, Lateral ventricle, Third ventricle, Semiannular sulcus, and Lateral fissure (Fig. 1). Practically, using the original brain outer surface (Fig. 2 (a)) of the atlas in Fig. 1, the simplified outer surface in Fig. 2 (b) is extracted manually by experienced neurosurgeons. Also, the brain outer surface of the patient is simplified. Both the simplified outer surfaces are smoothed by applying a median-like filter to the points on the surfaces (Fig. 2 (c)).

B. Initial landmark selection

To find the correspondence between the atlas and the patient brain, the initial landmarks are selected by two ways. The first selection uses the simplified brain outer surface and the contours of the detectable structures from MR images. The detectable structures are putamen, temporal horn of lateral ventricle, and caudate neucleus (Fig. 1). The boundaries of these structures are extracted manually by the experienced neurosurgeon. This process costs at most 20 minutes per a

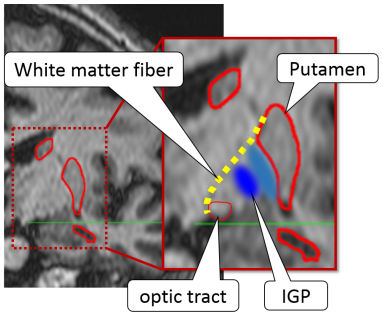

Fig. 3. Spatial relationship between the white matter fiber and other internal structures.

MR image. In the first selection, the points at parts of high curvature are automatically chosen from the simplified brain outer surface and the contours of the detectable structures. The red points in Fig. 2(d) are the chosen points. Referring the chosen points, the small number of the initial landmarks is selected manually from the contours of the simplified brain outer surface and the detectable structures of the atlas.

The second selection of the landmarks is derived from the geometrical relationship among the internal structures in the human brain. As shown in Fig. 3, white matter fiber run between putamen and optic tract. In other words, EGP and IGP lie below white matter fiber. Here, the curve of the white matter fiber is approximated by the straight line, called the Pu-Opt line, connecting between putamen and optic tract. The endpoints of the line are used as the initial landmarks. Moreover, the partial contour of the optic tract is included in the brain outer surface. Considering that the optic tract shape is an ellipse, the whole contour of the optic tract is estimated based on its known partial contour. The initial landmarks are selected from the estimated whole contour of optic tract.

In the same way of selecting the initial landmarks, the corresponding point of the initial landmarks are selected manually from the patient brain. All the initial landmarks from the atlas are shown as the blue circles in Fig. 2(e). Using the patient image in Fig. 4(a), the corresponding points selected from the patient brain are shown in the circles in Fig. 4(b).

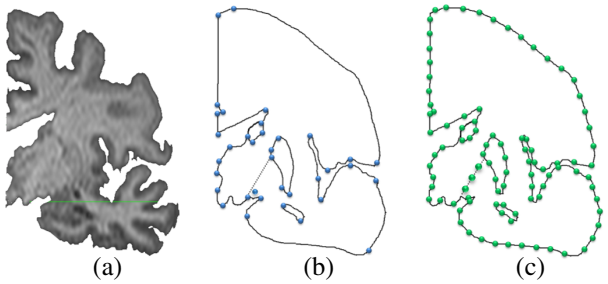

Fig. 4. Landmarks from a patient brain: (a) a patient brain image; (b) the corresponding points of the initial landmarks in Fig. 2(e); (c) final landmarks.

C. Automatic landmark generation

Using the selected initial landmarks, we find the correspondence between the points of the atlas and the patient brain. Let us denote by $\boldsymbol{p}_m = \boldsymbol{v}_i$ and $\boldsymbol{p}_{m+1} = \boldsymbol{v}_j$ $(j = i + N_m)$ the two adjacent initial landmarks on the contour of the same structure in the atlas. When there are N_m points between $\boldsymbol{v}_i$ and $\boldsymbol{v}_j$ on the contour, the k-th point $(i \le k \le j = i + N_m - 1)$ is denoted as $\boldsymbol{v}_k$. When the corresponding points $\boldsymbol{q}_m = \boldsymbol{u}_s$ and $\boldsymbol{q}_{m+1} = \boldsymbol{u}_t$ of $\boldsymbol{p}_m$ and $\boldsymbol{p}_{m+1}$ are given, the point $\boldsymbol{v}_k$ corresponds to the point $\boldsymbol{u}_h$ between $\boldsymbol{u}_s$ and $\boldsymbol{u}_t$ satisfying

$$h = s + floor\left[\frac{N_i}{M_s}(k-i)\right] \tag{1}$$

where M_s is the number of the points between $\boldsymbol{u}_s$ and $\boldsymbol{u}_t$. The function $floor[x]$ returns the greatest integer that is less than or equal to x.

Applying the above process to all the contours in the atlas, there are many correspondences between the atlas and the patient brain. In the atlas deformation, the use of many landmarks has the potential to improve the fitness of the deformed atlas to the patient brain. On the contrary, this results in the increase of the computational time. Therefore, the final landmarks are selected from the points to reduce the computational time. Fig. 2(f) and Fig. 4(c) show the final landmarks of the atlas and the patient brain.

D. Atlas deformation by FEM

One deformation method using RBF is Thin Plate Spline (TPS) [6] which allows to both deform a given object smoothly and move several points toward their specific locations. However, the problem with TPS is that it often generates unnatural deformation when many points with the latter constraint are used.

Here, finite element method (FEM) is a well-known technique for accurately modeling the behaviors of continuous objects. Compared with other deformation techniques, FEM can achieve a more physically realistic deformation for deformable objects with linear and non-linear material properties. In addition, the global and local deformation are easily controlled by changing the governing equations of the object to be deformed and the setting of several parameters in FE analysis. Owing to these benefits, our method deform the atlas by FEM although the FE analysis is very time-consuming.

Using the points in the atlas, the FE mesh model of the atlas is obtained by generating triangular elements. We assume that the brain deformation is elastic. The elastic model in our method includes two paramters: by Young's modulus and Poisson's ratio. The suitable values of these parameters are determined through preliminary experiments.

TABLE I

SPECIFICATION OF MRI

MRI system	PHILIPS Achieva 1.5T SE
Sequence	T1-weighted 3D turbo gradient echo
TR	6.7 msec
TE	3.3 msec
Acquired voxel size	1 × 1 × 2 mm
Reconstructed voxel size	0.5 × 0.5 × 1 mm
FOV	256 × 216 × 145 mm
Total scan duration	326 sec

III. EXPERIMENTAL RESULT

To verify the applicability of our proposed method, we made the experiments to estimate the locations of IGP and EGP from 10 MR images of patient brains. Table I summarizes the specification of MRI parameters. The proposed method is compared with six methods (Table II). The proposed method and Methods B-E use the simplified brain outer surface described in Sec. II-A while the original brain outer surface is used in Methods F and G. In the initial landmark selections, all the method use the brain outer surface, and the methods except Methods E and G uses the contour of putamen, temporal horn of lateral ventricle, and caudate neucleus (Sec. II-B). In addition, the proposed method and Method C select the initial landmark from Pu-Opt line. To deform the atlas, the proposed method and Method B uses FEM while TPS is employed in the other methods. FEM is made by a commercial softwear ”MSC.Marc”. Using this softwear, it takes 4-9 hours to estimate the atlas deformation.

To evaluate the methods, the ground truths of EGP and IGP is employed which are obtained by tracing their contours on the patient MR image by one experienced neurosurgeon. The accuracy of the estimated structures in the deformed atlas is evaluated by Dice similarity coefficient (DSC) which measures the spatial overlap between given two regions R_1 and R_2:

$$DSC = \frac{2|R_1 \cap R_2|}{|R_1| + |R_2|} \tag{2}$$

where $|R|$ is the area of a region R. When DSC is close to the value of one, the two regions R_1 and R_2 overlap completely.

The seventh and eighth columns in Table II show mean and standard deviation of DSC for EGP and IGP. The paired t-test statistical method is applied to the DSC results. The two symbols ”$*$” and ”†” in the columns indicate that there is the statistically significant differences ($p \le 0.05$) from the proposed method and Method B.

The mean DSC of estimated IGP and EGP using our method is the highest among the other methods. The sixth

TABLE II

COMPARISON OF THE PROPOSED METHOD WITH SIX OTHER METHODS.

	Brain outer surface	Internal structures		Deformation Method	Average Num. initial landmarks	Mean and Standard deviation of DSC	
		Pu, Cd, TLV	Pu-Opt line			IGP	EGP
Proposed Method	Simplified	◯	◯	FEM	40	0.700±0.116	0.873±0.060
Method B	Simplified	◯	×	FEM	35	0.640±0.101	0.844±0.041
Method C	Simplified	◯	◯	TPS	40	0.637±0.088	0.818± 0.055
Method D	Simplified	◯	×	TPS	35	0.554±0.077*	0.800±0.045*,†
Method E	Simplified	×	×	TPS	24	0.529±0.201*	0.574±0.139*,†
Method F	Original	◯	×	TPS	63	0.518±0.106*,†	0.787±0.064*,†
Method G	Original	×	×	TPS	52	0.274±0.205*,†	0.289±0.225*,†

*, †: $p \leq 0.05$ significant difference from our method and Method B, respectively.

column in Table II indicates the average number of the landmarks used in the atlas deformation. Since the original brain outer surface used in Method F and G has complex shape, more landmarks are needed to fit the atlas to the patient brain. Nevertheless, compared with the two method, the proposed method and Methods B-E, which select the landmarks from the simplified outer surface, reduce the number of the landmarks, and their estimation accuracy is improved. The reduction of the landmarks leads to speed up the deformation process. Comparing method E and G, and method D and F, the method using the simplified outer surface is superior to the method using the original outer surface in term of the accuracy of estimating IGP and EGP.

The third and fourth columns of the table indicate whether the features are used (◯) or not (×). Comparing with the methods using the same deformation, the accuracy of estimating IGP and EGP is improved better according to the increase of the number of the internal structures used in the estimation. Practically, the difference between our method and Method D-G is statistically significant. This is because our method uses the additional constraint, Pu-Opt line. Also, the effectiveness of Pu-Opt line is drawn from the comparisons of the pairs of our method and Method B, and Method C and Method D.

The DSC values of the proposed method and Method B are superior to those of Method C and D, respectively. The fifth column in the table indicates the deformation method. FEM used in the proposed method and Method B deforms the atlas based on a physical model, and retrain the occurrence of an unnatural deformation which TPS often generates.

The contour lines of ground truth are superimposed on the experimental results estimated by our proposed method (Fig. 5). In this case, the DSC of IGP and EGP are 0.829 and 0.922. Our method assumes that EGP and IGP lie below white matter fiber. However, In the atlas used in the experiment, the parts of IGP and EGP exist above white matter fiber. Therefore, our method estimate the internal structures robustly and reliably by a more suitable atlas satisfying our assumption.

IV. CONCLUSIONS

We proposed a new method for estimating the internal structures of a patient brain by deforming the brain atlas using FEM. In the proposed method, the brain outer surface is approximated by smoothing the whole outer surface while keeping the shape of the major sulci and gyri. Using FEM, the atlas is deformed based on the correspondence between the outer surface and the internal structures of the brain. From the experimental results, our method can estimate the regions of IGP and EGP with reliable accuracy.

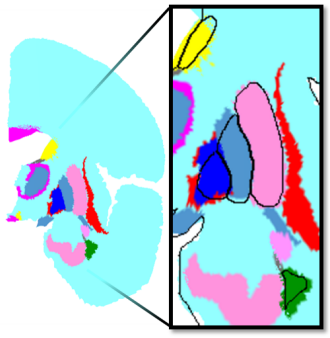

Fig. 5. The estimated internal structures by our method compared with their ground truth.

Our future work includes the extension of the proposed method to 3D volume model of brain atlas. Moreover, since FEM is very time-consuming, the speed up of the deformation process by FEM is needed.

REFERENCES

[1] R. O'orman, K. Shmueli, K. Ashkan, M. Samuel, D. Lythgoe, A. Shahidiani, S. Wastling, M. Footman, R. Selway, and J. Jarosz, "Optimal mri methods for direct stereotactic targeting of the subthalamic nucleus and globus pallidus," *European Radiology*, vol. 21, no. 1, pp. 130–136, 2011.

[2] M. J. K., V. Thomas, and P. George, *Atlas of the human brain*, 3rd ed. Academic Press, 2008.

[3] M. S. Buchsbaum, J. H. Fallon, T.-C. Wei, S. Guich, J. Spiegel-Cohen, M. Hamilton, and C. Tang, "A method of basal forebrain anatomical standardization for functional image analysis," *Psychiatry Research: Neuroimaging*, vol. 84, no. 2-3, pp. 113 – 125, 1998.

[4] M. Ortega, M. Juan, M. Alcaniz, J. Gil, and C. Monserrat, "Deformable brain atlas: Validation of the location of subthalamic nucleus using t1-weighted MR images of patients operated on for parkinsonś," *Computerized Medical Imaging and Graphics*, vol. 32, no. 5, pp. 367 – 378, 2008.

[5] K. A. Ganser, H. Dickhaus, R. Metzner, and C. R. Wirtz, "A deformable digital brain atlas system according to talairach and tournoux," *Medical Image Analysis*, vol. 8, no. 1, pp. 3 – 22, 2004.

[6] F. Bookstein, "Biometrics, biomathematics and the morphometric synthesis," *Bulletin of Mathematical Biology*, vol. 58, no. 2, pp. 313–365, 1996.